Phase behavior of casein micelles/exocellular polysaccharide mixtures : experiment and theory

Phase behavior of casein micelles/exocellular polysaccharide mixtures: Experiment and theory

R. Tuinier and C. G. de Kruif

Citation: The Journal of Chemical Physics **110**, 9296 (1999); doi: 10.1063/1.478851
View online: http://dx.doi.org/10.1063/1.478851
View Table of Contents: http://scitation.aip.org/content/aip/journal/jcp/110/18?ver=pdfcov
Published by the AIP Publishing

Phase behavior of casein micelles/exocellular polysaccharide mixtures: Experiment and theory

R. Tuinier
NIZO Food Research, P.O. Box 20, 6710 BA Ede, The Netherlands and Laboratory for Physical Chemistry and Colloid Science, Department of Biomolecular Sciences, Wageningen Agricultural University, Dreijenplein 6, 6703 HB Wageningen, The Netherlands

C. G. de Kruif[a)]
NIZO Food Research, P.O. Box 20, 6710 BA Ede, The Netherlands

(Received 14 October 1998; accepted 26 January 1999)

Dispersions of casein micelles and an exocellular polysaccharide (EPS), obtained from *Lactococcus lactis* subsp. *cremoris* NIZO B40 EPS, show a phase separation. The phase separation is of the colloidal gas–liquid type. We have determined a phase diagram that describes the separation of skim milk with EPS into a casein-micelle rich phase and an EPS rich phase. We compare the phase diagram with those calculated from theories developed by Vrij, and by Lekkerkerker and co-workers, showing that the experimental phase boundary can be predicted quite well. From dynamic light scattering measurements of the self-diffusion of the casein micelles in the presence of EPS the spinodal could be located and it corresponds with the experimental phase boundary. [S0021-9606(99)50816-7]

I. INTRODUCTION

Solutions containing both proteins and polysaccharides may exhibit phase separation. This was first reported in 1896 by Beijerinck, who observed a phase separation after mixing aqueous solutions of gelatin and starch.[1] Milk proteins and polysaccharides also exhibit incompatibility, as was reported for example by Tolstoguzov[2,3] and Antonov *et al.*[4] During the production process of dairy products polysaccharides and proteinaceous particles are often combined. Mixing proteins and polysaccharides also takes place during the fermentation process where exocellular polysaccharides (EPSs) by lactic acid bacteria are produced *in situ* in products such as yogurt. In yogurt the EPS seems to play an important role and is responsible for the threadlike pouring behavior of some types of yogurt. Previously, we have characterized physical properties of an EPS produced by *Lactococcus lactis* subsp. *cremoris* strain NIZO B40, which has a number-averaged molar mass of 1.47×10^6 g/mol and a number-averaged radius of gyration of 86 nm, and has a small polydispersity.[5]

Low-heat skim milk was chosen as milk protein system. Skim milk can be regarded as a 10% (v/v) suspension of casein micelles, which are association colloids with a diameter of 200 nm, in an aqueous (continuous) phase containing other but very small (<5 nm) components (salts, lactose, and whey proteins). Casein micelles can be considered as hard spheres as follows from diffusion[6] and rheology measurements.[7]

B40 EPS, when added to skim milk above a certain concentration, induces phase separation, as will be shown in Sec. IV. When the continuous phase of skim milk is mixed with B40 EPS (further denoted as EPS) nothing happens. This indicates that the interactions between casein micelles and EPS are responsible for the observed phenomena.

The phase separation is caused by the so-called depletion type of interaction and is also referred to as depletion flocculation. A better term would be segregative behavior. An early experimental observation of phase separation driven by depletion interaction was reported by Traube,[8] who investigated the effect of adding polymer molecules on creaming of natural rubber. About ten years later the depletion phenomenon was used in practice for the concentration of natural latex by plant polysaccharides, as described by Vester.[9] Asakura and Oosawa[10] gave a theoretical expression for the depletion interactions between two flat plates. Vrij[11] developed a thermodynamic model for the depletion in a mixture of colloidal spherical particles and nonadsorbing polymer molecules. De Hek and Vrij[12] observed phase separation in mixtures of colloidal silica spheres and polystyrene polymers, and the theory of Vrij[11] reasonably predicts the limiting polymer concentration for this system. Lekkerkerker[13] also developed a more sophisticated theory for depletion interaction using a different thermodynamic route. More recently, Lekkerkerker *et al.*[14] and Poon and Pusey[15] extended and refined this theoretical description.

In this paper it is shown that EPSs do not adsorb onto casein micelles and induce depletion flocculation in skim milk. We will compare two theoretical methods which allow the calculation of the phase line. An instability condition for a simpler adhesive hard sphere model (2.2) will also be given in order to locate a phase boundary from dynamic light scattering measurements. In this paper we show that phase diagrams calculated from depletion theories are consistent with the experimental phase diagram of a biological system containing casein micelles and EPS, indicating the practical relevance of depletion interaction.

[a)]Author to whom all correspondence should be addressed; electronic mail: dekruif@nizo.nl

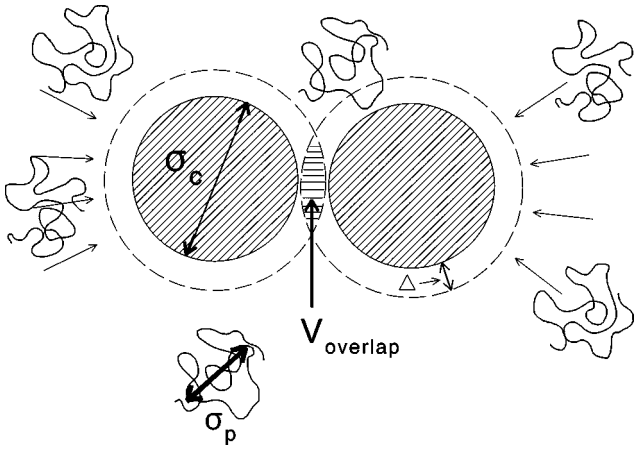

FIG. 1. Schematic picture of the depletion interaction mechanism. The colloidal spheres with diameter σ_c are pushed together by the unbalanced osmotic pressure as exerted by the polymer molecules with diameter σ_c.

II. THEORY

A. Depletion interaction theories

1. Vrij theory

A schematic picture of colloidal spherical particles dispersed in a solution of nonadsorbing polymer molecules is sketched in Fig. 1. The polymer molecules, with an effective diameter σ_p (twice the depletion layer thickness Δ) are assumed to be freely permeable toward one another (θ solvent) but are hard spheres for the colloids with diameter σ_c. Vrij[11] derived that then the attractive interparticle potential between two spherical colloidal particles, which behave as hard spheres toward one another, is proportional to the overlap volume V_{overlap} and to the osmotic pressure of the polymer solution Π_p. For the osmotic pressure of the polymer solution Vrij used the limiting Van 't Hoff's law:

$$\Pi_p = c_p RT/M, \tag{1}$$

where c_p is the polymer concentration, R the gas constant, T the temperature, and M the molar mass of the polymer. The overlap volume depends on the distance between the centers of the particles r:

$$V_{\text{overlap}}(r) = \frac{1}{6}\pi(\sigma_c+\sigma_p)^3\left[1-\frac{3r}{2(\sigma_c+\sigma_p)}+\frac{r^3}{2(\sigma_c+\sigma_p)^3}\right]. \tag{2}$$

This expression applies for $\sigma_c < r < (\sigma_c+\sigma_p)$. Now the depletion interaction potential of Vrij is given by[11]

$$\begin{aligned} U(r) &= +\infty, \quad 0<r<\sigma_c \\ &= \Pi_p V_{\text{overlap}}(r), \quad \sigma_c \leqslant r \leqslant (\sigma_c+\sigma_p) \\ &= 0, \quad r>(\sigma_c+\sigma_p). \end{aligned} \tag{3}$$

Given the pair potential the equilibrium properties of the system can be evaluated using statistical mechanics.[16] If the polymer-induced attraction between two particles becomes strong enough the system tends to phase separate into a colloid-rich and polymer-rich phase.[14] The calculation of the binodal in a statistical mechanical way is possible but rather involved. Simpler is a calculation of the spinodal the osmotic compressibility $\partial\Pi_c/\partial\phi$ becomes zero:[16]

$$\frac{\partial\Pi_c}{\partial\phi}=0. \tag{4}$$

The spinodal usually lies very close to the binodal and therefore the spinodal can also be taken as an estimation of the phase boundary. The virial expansion of the osmotic pressure of colloids is[17]

$$\frac{\Pi_c V_c}{k_B T} = \phi + B_2\phi^2 + B_3\phi^3 + \cdots, \tag{5}$$

where $V_c(=\pi\sigma_c^3/6)$ is the particle volume of the colloidal spherical, B_2 is the second, and B_3 the third osmotic virial coefficient. For low volume fractions ($\phi<0.2$) B_3 and higher-order terms can be neglected. Combining Eqs. (4) and (5) gives the value B_2^{sp} at the spinodal for a given volume fraction:

$$B_2^{\text{sp}} = -\frac{1}{2\phi^{\text{sp}}}, \tag{6}$$

where ϕ^{sp} is the volume fraction at the spinodal. The second virial coefficient can be measured in the one-phase region at a given ϕ. On addition of polymer, B_2 will decrease due to attractions. From statistical mechanics a relation between $U(r)$ and B_2 can be derived:[16]

$$B_2 = \frac{2\pi}{V_c}\int_0^\infty r^2(1-e^{-U(r)/k_BT})dr, \tag{7}$$

which gives $B_2=4$ for the hard sphere interaction potential. For depletion interactions, we calculate B_2 from Eq. (7) by taking $U(r)$ from Eq. (3). This then yields B_2, which becomes negative for sufficiently high polymer concentrations, eventually leading to spinodal demixing. So, for a mixture with a certain volume fraction ϕ of colloidal spheres with diameter σ_c the effect of nonadsorbing polymer molecules on B_2^{sp} can be calculated. This yields the limiting polymer concentration and by doing this at various values of ϕ the phase diagram can be calculated.

Since in the approach of Vrij only pair interactions are involved, which is incorrect above the dilute regime, we have also used an alternative thermodynamic route which takes into account many particle interactions to calculate the spinodal with the interaction potential for the depletion interaction given in Eq. (3). From Eq. (4) we know that the spinodal corresponds to the point where the osmotic compressibility $\partial\Pi_c/\partial\phi$ equals zero. Therefore use can be made of the relation between the structure factor of a colloidal dispersion $S(Q)$, which can be measured with scattering techniques. The osmotic compressibility and $S(Q)$ are related as follows:

$$S(Q=0) = kT\frac{\partial\rho}{\partial\Pi}, \tag{8}$$

where $\rho=N_c/V$ is the number density, with N_c the number of particles in a volume V, which is related to the volume fraction by $\phi=N_cV_c/V$. The scattering wave vector Q

equals $4\pi n \sin(\theta/2)/\lambda_0$, where n is the refractive index, θ is the angle under which the scattered intensity is detected, and λ_0 is the wavelength *in vacuo*. Comparison with Eq. (4) shows that the condition $S(Q=0)^{-1}=0$ gives the spinodal. The structure factor $S(Q)$ is defined as the Fourier transform of $g(r)$:

$$S(Q)=1+4\pi\rho\int_0^\infty r^2[g(r)-1]\frac{\sin(Qr)}{Qr}dr, \tag{9}$$

where r is the distance between the centers of any two randomly chosen particles, say particles 1 and 2. In order to calculate $S(Q)$ one thus needs an expression for the radial distribution function $g(r)$. The integral equation of Ornstein and Zernike (the OZ equation) gives the total correlation function $h(r)$:[18]

$$h(r)=c(r_{12})+\rho\int c(r_{13})h(r_{23})dr_3, \tag{10}$$

which makes it possible to solve for $g(r)=h(r)+1$ when one has an appropriate closure relation for $c(r_{12})$, the direct correlation function. The OZE defines $g(r)$ as the sum of the direct effect of particle 1 on particle 2 and an indirect effect of 1 on 2 in which all other particles are involved. We have used the hypernetted chain (HNC) closure relation:[19]

$$c(r)=h(r)-\ln(g(r)-U(r)/k_BT). \tag{11}$$

We applied a mathematical solution procedure developed by Gillan[20] to solve Eqs. (10) and (11). We can insert Eq. (3) into the HNC closure and subsequently calculate $g(r)$ and $S(Q)$ by using Eqs. (10) and (9). Hence, $S(Q=0)$ can be obtained as a function of c_p, which makes it possible to calculate the spinodal [the polymer concentration for which $1/S(Q=0)$ equals zero].

In the foregoing the depletion layer thickness Δ was left unspecified. Usually, it is identified with the radius of gyration of the polymer molecules: $\Delta=R_g=\sigma_p/2$. De Hek and Vrij[12] numerically calculated the distance r where the particles just start to attract one another and found $\sigma_p \approx 2.25R_g$, which confirms that $\Delta\approx R_g$. Calculations of Fleer *et al.*[21] for concentrations below overlap give $\Delta\approx R_g$, which also corroborates the general assumption that the radius of gyration is a good measure of the depletion layer thickness in dilute solutions. Fleer *et al.* also calculated the decrease of Δ above coil overlap, but since in our case c_p is below the overlap threshold we do not need these expressions.

In order to illustrate the main trends some model predictions as calculated with the theory of Vrij[11,12] are given in Fig. 2. Results are calculated for a mixture of colloidal particles with a radius of 100 nm ($\sigma_c=200$ nm) and polymer molecules with a molar mass of 10^3 kg/mol and three different radii of gyration: 30, 60, and 90 nm ($\sigma_p=60$, 120, and 180 nm), respectively, corresponding to varying the flexibility of the chains. Increasing ϕ gives a lower limiting polymer concentration since according to Eq. (6) the product $\phi \cdot B_2^{sp}$ is a constant. This indicates that a less negative value of B_2^{sp}, and hence a lower polymer concentration, is required at higher ϕ. By comparing the results for the various sizes of the polymer molecules, we observe a decreasing spinodal demixing curve with increasing depletion layer thickness (larger polymer molecules). This indicates that when the polymer chains are more stiff, leading to a larger R_g, they will have a stronger tendency to induce phase separation by the depletion interaction mechanism.

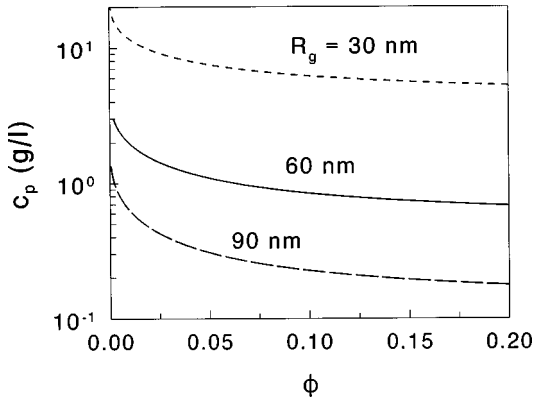

FIG. 2. Phase lines as calculated with the theory of Vrij (Refs. 9 and 11) for colloidal spheres with a diameter of 200 nm and polymer molecules with a molar mass of 1000 kg/mol and radii of gyration (R_g) as indicated.

2. Lekkerkerker theory

Another way of calculating the phase lines was developed by Lekkerkerker and co-workers. The approach is based upon a grand canonical statistical mechanical description of hard spheres in the presence of freely interpenetrable coils. Lekkerkerker *et al.*[14] derived expressions for both the osmotic pressures and the thermodynamic potentials of the colloidal suspension for the fluid as well as for the crystal phases in order to predict the phase behavior of polymer–colloid mixtures by calculation of the binodal. The polymer concentration acts as perturbation parameter.

a. Fluid phase. For the fluid phase a dimensionless osmotic pressure Π_f is expressed as:

$$\Pi_f=\frac{\phi}{1-\phi}+3\left(\frac{\phi}{1-\phi}\right)^2+3\left(\frac{\phi}{1-\phi}\right)^3+\frac{c_p^R\pi\sigma_c^2}{6M\zeta^3}\left(\alpha-\frac{d\alpha}{d\phi}\right), \tag{12}$$

where c_p^R is the overall polymer concentration in the reservoir. The fraction α is the fraction of the total volume which is accessible to the polymer molecules, and $\zeta=\sigma_p/\sigma_c$ is the size ratio of the polymer molecules relative to the colloidal spheres. The macroscopic polymer concentration equals $\alpha \cdot c_p^R$. The free volume fraction α can be calculated from:[14,15]

$$\alpha=(1-\phi)\exp\left[-A\frac{\phi}{1-\phi}-B\left(\frac{\phi}{1-\phi}\right)^2 C\left(\frac{\phi}{1-\phi}\right)^3\right], \tag{13}$$

with $A=3\zeta+3\zeta^2+\zeta^3$, $B=4.5\zeta^2+3\zeta^3$, and $C=3\zeta^3$. Equation (13) reduces to $\alpha=1-\phi$ for $\zeta\to 0$. The first three terms on the right-hand side of Eq. (12) are derived from the Percus–Yevick equation of state[22] and the fourth term is a perturbation factor arising from the presence of the polymer molecules. For the thermodynamic potential μ_f of colloidal spheres in the fluid phase Lekkerkerker *et al.*[14] derived the following equation:

$$\frac{\mu_f}{k_BT}=\ln\left(\frac{\phi}{1-\phi}\right)+7\left(\frac{\phi}{1-\phi}\right)+\frac{15}{2}\left(\frac{\phi}{1-\phi}\right)^2+3\left(\frac{\phi}{1-\phi}\right)^3-\frac{c_p^R\pi\sigma_c^2}{6M\zeta^3}\frac{d\alpha}{d\phi_c}, \tag{14}$$

which has the same physical origin as Eq. (12).

b. Solid phase. For the crystal or solid phase, equations analogous to Eqs. (12) and (14) can be derived. For the osmotic pressure, a simplified version of the equation of state of Hall[23] is used:

$$\Pi_s=\frac{\phi}{1-\frac{\phi}{\phi_{\rm cp}}}+\frac{c_p^R\pi\sigma_c^2}{6M\zeta^3}\left(\alpha-\frac{d\alpha}{d\phi}\right), \tag{15}$$

where ϕ is now the volume fraction of colloidal particles in the solid phase and $\phi_{\rm cp}$ is the volume fraction at closest packing ($=\pi\sqrt{2}/6$). The thermodynamic potential in the solid phase is given by:

$$\frac{\mu_s}{k_BT}=2.1306+3\ln\left(\frac{\phi}{1-\frac{\phi}{\phi_{\rm cp}}}\right)+\frac{3}{1-\frac{\phi}{\phi_{\rm cp}}}-\frac{c_p^R\pi\sigma_c^2}{6M\zeta^3}\frac{d\alpha}{d\phi}, \tag{16}$$

where the constant cannot be calculated analytically. The value 2.1306 given above is taken from computer simulations of Frenkel and Ladd[24] and is consistent with experimental values for $\phi=0.494$ and 0.545 at the fluid–crystal transition of a suspension of hard spheres.

Subsequently, the phase behavior can be calculated from the conditions $\Pi_f=\Pi_s$ and $\mu_f=\mu_s$. This gives two sets of equations with two unknowns, ϕ's for the volume fractions of colloids in the coexisting phases, which can be solved numerically. The model described above makes it is possible to calculate the phase behavior of polymer–colloid mixtures. The coexisting phases which can be found are fluid–solid, and above approximately $\zeta=0.3$ gas–liquid, gas–solid, and gas–liquid–solid since the fluid phase then also exhibits a gas–liquid transition.

B. Adhesive hard sphere model

For skim milk it has been shown[6,7] that casein micelles can be treated as hard spheres under the conditions relevant for this study. When hard spheres become sufficiently attractive a (colloidal) fluid–solid transition takes place which can be regarded as a phase separation. Casein micelles become attractive when EPS is added to skim milk. We use the adhesive hard sphere (AHS) model in order to make a connection between dynamic light scattering experiments and the attraction between colloidal particles.

An interaction potential profile for adhesive spheres has been proposed by Baxter[25] as a square well potential with an infinitely narrow width ($\delta\to 0$):

$$\begin{aligned}\frac{U(r)}{k_BT}&=+\infty, \quad 0<r<\sigma_c,\\ &=\ln[12\tau_B\delta/(\sigma_c+\delta)], \quad \sigma_c\leqslant r\leqslant(\sigma_c+\delta)\\ &=0, \quad r>(\sigma_c+\delta),\end{aligned} \tag{17}$$

where τ_B is the Baxter parameter ($0<\tau_B<\infty$) and τ_B^{-1} is a measure of the attraction between the spheres. A prerequisite for applying the Baxter potential is that the term $\tau_B\delta$ has to remain finite. The experimentally accessible parameter from light scattering and osmotic pressure measurements is B_2. Combining Eqs. (7) and (17) gives:

$$B_2=4-\frac{1}{\tau_B}. \tag{18}$$

Using Baxter's approach Watts *et al.*[26] showed that τ_B can be directly related to the volume fraction at the spinodal $\phi^{\rm sp}$. For a volume fraction lower than 0.12, Penders and Vrij[27] simplified the expressions of Watts *et al.*[26] to:

$$\tau_B=\frac{\phi^{\rm sp}}{1-\phi^{\rm sp}}\left(\sqrt{\frac{1+\frac{1}{2}\phi^{\rm sp}}{3\phi^{\rm sp}}}-1\right). \tag{19}$$

For higher values of ϕ, the PY theory can be used.[22,27] Equation (19) allows us to calculate the volume fraction at which decomposition takes place at a certain adhesiveness. So, when τ_B is determined the spinodal can be calculated. Although strictly speaking the AHS model is not correct for our system we apply it here since it provides a theoretical framework which allows us to describe the phase separation in terms of τ_B values, which can be calculated from for instance transport properties. The way τ_B is related to the self-diffusion coefficient is treated in Sec. II C.

C. Phase separation from self-diffusion

Previously[28] we have measured τ_B of skim milk–EPS mixtures by dynamic light scattering. We calculated Baxter parameters from the measured self-diffusion coefficients by applying the following expression from Cichocki and Felderhof:[29]

$$\frac{D_s}{D_0}=1-\left(1.832+\frac{0.295}{\tau_B}\right)\phi, \tag{20}$$

where D_s is the self-diffusion coefficient and D_0 is its value at $\phi\to 0$. By calculating τ_B values from Eq. (20), $\phi^{\rm sp}$ can subsequently be obtained from Eq (19). Hence, scattering data allow calculation of the phase boundary.

However, in the approach given above the viscosity increase due to the addition of B40 EPS to the continuous phase has been neglected. Previously, we have shown[30] that the (zero-shear) specific viscosity $\eta_{\rm sp}=\{\eta_0-\eta_s\}/\eta_s$ (where η_0 is the zero-shear solution viscosity and η_s the solvent viscosity) of polysaccharide solutions can be described as:

$$\eta_{\rm sp}=[\eta]c+\tfrac{1}{25}([\eta]c)^{3.5}, \tag{21}$$

where $[\eta]$ is the intrinsic viscosity of the polysaccharide solution. For EPS solutions with an ionic strength of 0.10 M, $[\eta]$ equals 3.2 m^3/kg. We assume the same value for skim

milk, where the ionic strength is close (0.08 M). Equation (21) indicates that the self-diffusion coefficient, which depends on the viscosity of the continuous phase, decreases when EPS is added to skim milk. We have to take this effect into account by applying a correction for the viscosity. However, for systems where the particle size is of the same order of magnitude as the polymer molecules it is not correct to simply replace the solvent viscosity with the viscosity of the continuous phase as measured macroscopically. The macroscopic viscosity overestimates the friction experienced by the colloidal particles.[31]

This phenomenon has been examined theoretically by Cukier[32] and De Gennes,[33] who found that relatively small colloidal particles tend to ''hunt for holes'' in polymer solutions. Microscopically a polymer solution can be regarded as a system containing obstacles (polymer chains) with a high resistance. Since the particles seek a path of minimum resistance, the viscosity as experienced by the diffusing particles is smaller than the macroscopic viscosity. The contribution of the polymers to the effective viscosity of the solution depends on the hydrodynamic colloidal particle–polymer size ratio, ζ_h, defined as R^P/R^S, where R^S refers to the hydrodynamic radius of the colloidal sphere and R^P to the effective radius of the polymer molecules. We are not aware of a theory which quantitatively describes the relation between the effective viscosity and ζ_h. In the limit $\zeta_h \rightarrow \infty$ the colloidal particles will only experience friction due to interaction with solvent molecules since the polymer molecules are so large that the particles can easily ''hunt for holes.'' When the value of ζ_h is very small the colloidal spheres cannot diffuse through the holes since the holes are too small. Therefore the particles will experience the macroscopic viscosity in the limit $\zeta_h \rightarrow 0$. At intermediate values for ζ_h the friction will lie in between the solvent and the polymer solution viscosity. Tentatively, we introduce an effective viscosity η_{eff} and propose that it depends as follows on ζ_h:

$$\frac{\eta_{\mathrm{eff}}}{\eta_s} = 1 + \eta_{\mathrm{sp}} \exp(-\zeta_h). \tag{22}$$

The solvent contribution is given by the first term on the right-hand side, and that of the solute by the second term. This equation describes the data in Ref. 31 reasonably well and gives a correct physical description for the limits.

For the sedimentation of colloidal particles through a polymer solution, Tong *et al.*[34] also found that for very large values of ζ_h the particles experience a much lower viscosity than that of the solvent with polymer molecules. The macroscopic viscosity of the solution is only experienced for $\zeta_h \rightarrow 0$. For R^P these authors use the correlation length ξ, which says that in the entangled region even small particles experience the macroscopic viscosity.

The approach given above will be used to account for the effect of the viscosity of the solution on the measured self-diffusion coefficient. Equation (20) can then be replaced by:

$$\frac{D_s}{D_0}\frac{\eta_{\mathrm{eff}}}{\eta_0} = 1 - \left(1.832 + \frac{0.295}{\tau_B}\right)\phi, \tag{23}$$

where η_{eff} is defined in Eq. (22).

III. EXPERIMENT

A. NIZO B40 EPS

NIZO B40 EPS was obtained after a fermentation and isolation process at the NIZO pilot plant as described elsewhere.[5] EPS was isolated using various filtration steps, freeze-dried, and used as such in this study.

B. Skim milk

Reconstituted skim milk was prepared as described in Ref. 7. The volume fraction of casein micelles in the reconstituted skim milk was determined by Jeurnink and De Kruif[7] as being 0.130.

C. Permeate

Skim milk permeate (i.e., the ''solvent'' of the casein micelles) was prepared from skim milk by a membrane filtration process. An Amicon hollow-cartridge HIMPO 1-43 membrane with a cutoff of 0.1 μm was used. The pH of the permeate was the same as that of the skim milk (6.60 ± 0.10).

D. Mixtures

The mixtures were prepared by dissolving EPS diluted in permeate and mixing this EPS–skim milk permeate solution with skim milk. All mixtures were studied at room temperature.

E. Preservative

Since phase separation was sometimes observed only after a few weeks we used anti-microbial agents (preservatives) in order to prevent growth of micro-organisms during the experiments. We used 0.02% (m/m) sodium ethylmercurithiosalicylate ($C_2H_5HgSC_6H_4COONa$-thiomersal, BDH Chemicals), with which we could not observe any bacterial growth or any pH changes for more than 6 weeks. In the absence of EPS, skim milk and permeate containing thiomersal were stable for months.

IV. RESULTS AND DISCUSSION

This section contains three parts. A description of the observed phase separation phenomena for the skim milk/permeate/EPS mixtures is given in Sec. IV A. Theoretical predictions of the phase diagram are presented in Sec. IV B and compared with the experiments. In Sec. IV C the Baxter parameters obtained from dynamic light scattering are used to calculate a phase diagram with the AHS model.

A. Observations and phase diagram

First, we dissolved EPS in low-heat skim milk permeate (skim milk without casein micelles). The highest EPS concentration studied was 10 g/ℓ since EPS is not soluble (on a practical time scale) at higher concentrations. This represents a practical concentration range since lactic acid bacteria produce EPSs up to concentrations of 0.5 g/ℓ. In permeate so-

lutions no phase separation could be observed for months when EPS was added. Apparently, whey proteins and EPS are fully compatible. Therefore we used permeate to dissolve EPS, after which this EPS–permeate solution was mixed with skim milk.

In this way the required final concentration c_p of EPS and the volume fraction ϕ of casein micelles could be adjusted independently in the range $0<c_p<10$ g/ℓ and $0<\phi<0.13$. Mixtures in this concentration range were prepared, stored, and studied at room temperature. For high EPS concentrations a two-phase system could be observed after several hours or, occasionally, after several days. The onset of phase separation occurred always within one week. In phase-separated systems the upper phase became clearer with time while the lower phase became highly turbid (white). In Fig. 3 a phase diagram is presented describing which mixtures demixed (filled circles) and which remained stable (open circles). The transition points (squares) are indicated for various ϕ values and a line which guides the eye represents the visually observed phase boundary. The EPS concentration at which the skim milk suspensions phase separate is rather low. The polymer overlap concentration c_p^*, which equals $3M_n/4\pi R_g^3 N_{\mathrm{av}}$, where M_n is the number-averaged molar mass and N_{av} Avogadro's number, is 0.92 ± 0.09 g/ℓ. This indicates that phase separation occurs in the dilute regime for casein volume fractions above $\phi \approx 0.03$.

In the course of time the upper layer becomes fully transparent. After about one week the upper phase has the same appearance as skim milk permeate. This indicates that the bottom layer is concentrated in casein micelles: their density is slightly higher than that of the permeate. We measured the EPS and casein concentration in the upper layer. For instance at $\phi=0.07$, samples with initial EPS concentrations of 0.75, 1.00 and 1.25 g/ℓ had an EPS concentration in the upper layer of 0.87, 1.03, and 1.33 g/ℓ, respectively, after phase separation. The volume fraction of casein micelles in the upper phase was always smaller than $\phi=0.01$. Systematically, there is a slight increase in the EPS concentration in the upper transparent layer while the caseins are highly concentrated in the lower phase. This is the first confirmation that the type of phase separation originates from depletion interaction and not bridging since polysaccharides and proteins are separated into two separate phases. If the mechanism would be bridging flocculation, polysaccharides and proteins are expected to concentrate in one of the two phases.

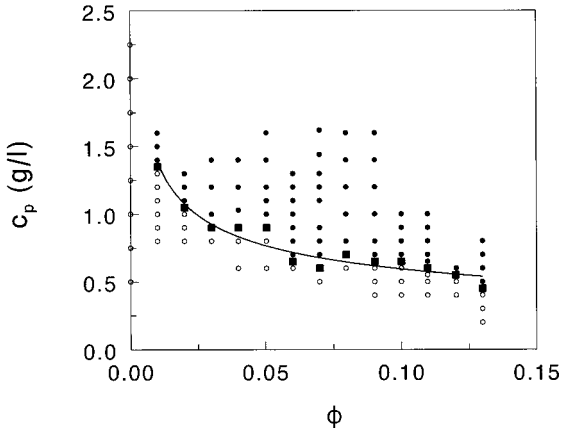

FIG. 3. Visually observed phase diagram for various EPS concentrations (c_p) and volume fractions of the casein micelles (ϕ). Indicated are the phase boundaries (squares), stable mixtures (open circles), and unstable mixtures (filled circles).

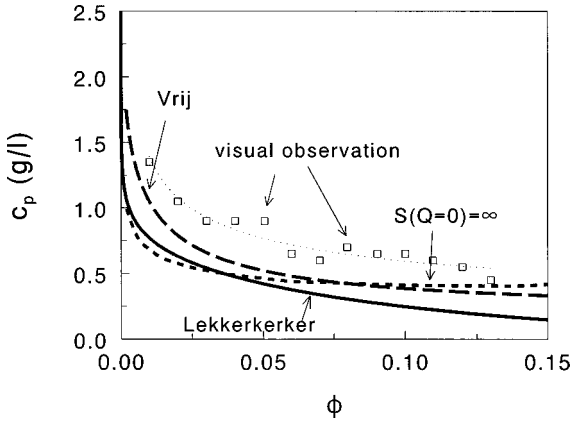

FIG. 4. Comparison of theoretically calculated phase lines with the visually observed phase boundary (squares), which is replotted as a dotted curve to guide the eye. The phase diagrams calculated with the various models are as indicated by Lekkerkerker (Ref. 14), Vrij (Ref. 9), and $S(Q=0)=\infty$ (obtained by combining Vrij's theory with Gillan's method—Ref. 20).

Another aspect which indicates that we are dealing with depletion flocculation is the fact that the flocculation is reversible. After initial phase separation the system can be mixed, after which it takes some time before the system becomes phase separated again. If a sample prepared with such a composition that it is located just above the phase separation threshold is shaken and subsequently diluted with skim milk permeate it remains stable. In the case of bridging flocculation, sedimentation or creaming is always irreversible. Moreover, in the case of bridging flocculation the limiting polymer concentration increases with increasing ϕ. Also this last characteristic of bridging was not found.

B. Theoretical description

1. The Vrij model

We have set the parameters in the model such that they comply with the experimental conditions for casein micelles and EPS: $\sigma_c=200$ nm, $M=1.47\times10^3$ kg/mol, and $\sigma_p=2R_g$, with $R_g=86$ nm for the radius of gyration. The resulting spinodal curve is plotted in Fig. 4 (long dashes), in which the phase boundary as observed visually is also given (symbols). The calculated phase line lies below the experimental phase boundary, but the difference is small. Also the shapes of the curves are similar. It should be noted that we calculated the phase boundary from independently measured characteristic parameters of the system; there is no data fitting.

As the next step we calculated the polymer concentrations for which $S(Q=0)$ goes to infinity as explained in Sec. II A 1. This was done by insertion of Vrij's interaction potential profile $U(r)$ [Eq. (3)] into Eq. (11). In order to solve $g(r)$ by combining Eqs. (10) and (11), we used Gillan's approach.[20] From the radial distribution function obtained in

this way $S(Q)$ was subsequently calculated with Eq. (9). By iteration we calculated at which polymer concentration $S(Q=0)$ approaches infinity and the resulting phase diagram (spinodal) is plotted in Fig. 4 (short dashes). In this way we implicitly accounted for multiple interactions, whereas Vrij's model is on the pair level. This phase line corresponds reasonably well to those calculated with the Lekkerkerker and Vrij models.

It must be realized that, except for the critical point the spinodal always lies above the binodal. Still, from the above it follows that a reasonable prediction can be made from the Vrij theory, which does not contain any adjustable parameters. The differences between experimental and theoretical phase boundary can further be explained by realizing that the casein micelles (and EPS) are not monodisperse. A model developed by Chu *et al.*[35] indicates that polydispersity of the colloidal particles weakens depletion interaction effects also and thus shifts the theoretical curves upwards.

2. Lekkerkerker theory

In the region where we observed phase separation visually the theory of Lekkerkerker *et al.*[14] predicts a colloidal gas–liquid transition. For our system with $\zeta=0.86$, we have calculated the phase diagram along the lines explained in Sec. II A 2. After calculating c_p from the overall reservoir concentration c_p^R by multiplying with α from Eq. (13), Eqs. (12) and (14)–(16) allow a calculation of the binodal. The calculated phase diagram is given for the relevant ϕ range in Fig. 4. This shows that the Vrij and Lekkerkerker models give approximately the same phase line. The comparison of theoretical predictions of the phase diagram with that of a model colloid–polymer mixture has already been done by Ilett *et al.*[36] In this paper it is shown however that the concepts of depletion interaction allow a quantitative description of mixtures of proteins and polysaccharides, illustrating the importance of depletion interaction in biological and food systems.

The calculations given above and in Sec. IV B 1 assume that the thickness of the depletion layer Δ is independent of c_p. Fleer *et al.*[21] developed a theory from which the decrease of Δ as a function of c_p can be calculated. In the Appendix we have calculated the $\Delta(c_p)$ dependence, which shows that Δ has a constant value in our relevant concentration region. This means that we do not have to incorporate a $\Delta(c_p)$ dependence in our calculations. Any effect would have shifted the calculated curves upward.

C. Phase diagram from self-diffusion

The diffusion coefficients were determined as described previously[28] for a series of polymer concentrations at various volume fractions. At every volume fraction we calculated the diffusion coefficient at the spinodal by combining Eqs. (19) and (20). For the moment we neglect viscosity corrections as described by Eqs. (22) and (23). Subsequently, we used the measured self-diffusion coefficients to infer at which polymer concentration the spinodal is situated. We plotted these spinodals in Fig. 5 (plus signs). The data are consistent with the experimental (observed) phase boundary although the phase boundary derived from the self-diffusion coefficient measurements is lower. The discrepancy may originate from the fact that just above the phase boundary nucleations of the new phase are extremely slow (and hence not observable). Another point is that the application of Baxter's sticky sphere model is hardly justified in view of the long range of the depletion interaction potential. Nevertheless, its use helps us to understand the phase behavior.

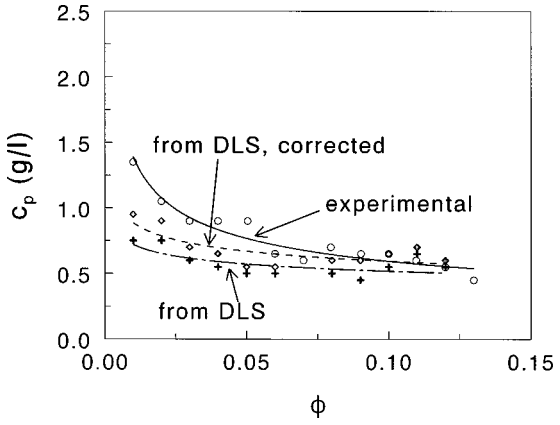

FIG. 5. Phase diagram with visually observed phase boundaries (open circles) and phase boundaries calculated from self-diffusion coefficient measurements. The results from the approach which uses Eq. (19) are given by the plus signs and those obtained with Eq. (22) are given by the diamonds. The curves are drawn to guide the eye.

Another aspect not fully accounted for is the viscosity experienced by the particles. We have calculated an effective viscosity from Eq. (22) and used Eq. (23) to correct the self-diffusion coefficient and, hence, the Baxter parameter τ_B. For the calculation of the effective viscosity we took the average end-to-end distance of EPS molecules as 211 nm as calculated from the radius of gyration for R^P. The data in Ref. 31 are described the best way if the end-to-end distance is taken for R^P. With $R^S=100$ nm this gives $\zeta_h\approx 2.11$. Then we used Eqs. (19), (22), and (23) to calculate the corresponding polymer concentration at the spinodal for every measured volume fraction. The result is plotted in Fig. 5 (diamonds); it is consistent with the observed phase behavior.

V. CONCLUSIONS

Phase separation caused by depletion interaction is observed when EPS is mixed with casein micelles. This polysaccharide is a nonadsorbing biopolymer with respect to casein micelles. Various theoretical models were compared with the observed phase threshold and gave good predictions of the stability limit. We were also able to calculate a phase diagram from dynamic light scattering experiments, and found it to be consistent with observations.

ACKNOWLEDGMENTS

This work was financially supported by the Association of Biotechnology Centers in the Netherlands (ABON). We thank the late Cyril Renaud for doing many experiments and remember him with gratitude. Professor H. N. W. Lekkerkerker and Gerrit Vliegenthart (Van't Hoff Laboratory, Utrecht University) are thanked for encouraging discussion and their help with the calculations of the phase boundary

with the Lekkerkerker model. Dr. E. Ten Grotenhuis, Dr. P. Zoon, and Dr. S. P. F. M. Roefs from NIZO Food Research are thanked for their interest. Professor M. A. Cohen Stuart and Professor G. J. Fleer from the Laboratory for Physical Chemistry and Colloid Science at Wageningen University are acknowledged for their support and critical reading of the manuscript.

APPENDIX

In this section we will give some results for the depletion layer thickness near a flat plate as can be obtained from self-consistent field (SCF) theory. In the theories of Vrij and Lekkerkerker it is assumed that changing the polymer concentration does not affect the depletion layer thickness Δ. De Gennes,[37] however, showed theoretically that the correlation length of concentration fluctuations ξ, which depends on the polymer concentration, is a good measure for Δ and gave the following scaling law for the concentration dependence of ξ:

$$\xi \sim c_p^{-m}, \tag{A1}$$

where m is a scaling parameter which is zero in the dilute regime and takes values of 3/4 (good solvent) or 1 (θ solvent) in the semidilute regime.

Hence, in the semidilute regime Δ is a decreasing function of c_p. This can be understood by realizing that at very high polymer concentrations the osmotic pressure Π_p becomes very high, which will push the polymer molecules into narrower gaps, giving smaller Δ values. Eventually, Δ becomes zero, which agrees with the observation that mixing colloidal spheres with polymer melts often does not give a phase separation.

In order to calculate the concentration dependence of Δ, the self-consistent field (SCF) theory of Scheutjens and Fleer[38,39] can be used. This theory is based upon a mean-field approach ($m=1/2$) and enables evaluation of the segment density profile of polymer molecules situated between two flat plates as a function of the plate separation at a given adsorption energy. In the SCF theory the polymer chains are described as weighted walks upon a lattice. The polymers are considered to behave as Kuhn chains.[40] For a Kuhn chain, the root-mean-square end-to-end distance, $\langle R^2\rangle^{1/2}$, follows from the number N_K of Kuhn segments and the length l_K of such a segment as:[41]

$$\langle R^2\rangle = l_K^2 N_K. \tag{A2}$$

For long chains the radius of gyration R_g equals $\sqrt{(\langle R^2\rangle/6)}$. However, real chains with N segments, each of length l, cannot be directly described as random-flight chains. The values for l and N can be translated to l_K and N_K by demanding equal contour lengths for the Kuhn chain and the real chain:

$$L \equiv l\,N = l_K N_K. \tag{A3}$$

When R_g has been measured, the quantity l_K can then be calculated from Eq. (A2) as $l_K=\langle R\rangle^2/L=6R_g^2/L$ and N_K follows as L/l_K.

Fleer *et al.*[21] studied the segment density profile for nonadsorbing polymer in a solution which is near $\chi=0.5$ (θ solvent), where χ is the Flory–Huggins segment–solvent interaction parameter, and obtained an analytical expression for Δ:

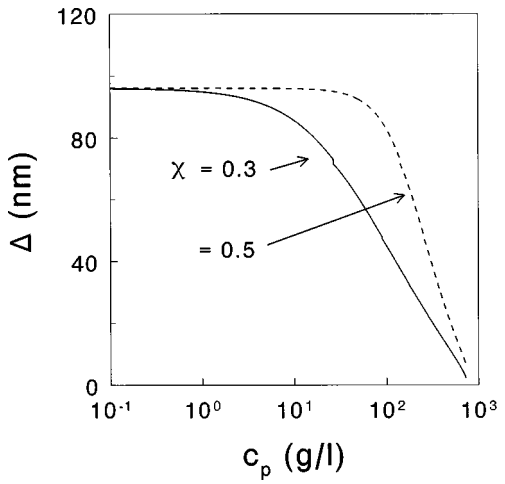

FIG. 6. Calculated depletion layer thickness Δ as a function of the polymer concentration according to Eq. (A4) for Flory–Huggins parameters as indicated in the plot.

$$\sin^2\left(\frac{\pi/2}{2\Delta/l_K+1}\right)=\left(\frac{1.95}{N_k}\right)\left(1+\frac{2.84}{\sqrt{N_k}}\right)-\ln(1-\phi_b)-2\chi\phi_b, \tag{A4}$$

where ϕ_b is the bulk volume fraction of polymer molecules. We calculated the $\Delta(c_p)$ dependence for $\chi=0.3$ and 0.5 which represent values usually found experimentally for polymers. The results are given in Fig. 6. For polymer molecules in a ''good'' solvent usually $\chi\approx 0.3-0.4$, leading to a result in between the curves drawn in Fig. 6. The calculations were performed with $N_K=153$ and $l_K=17$ nm, calculated from Eqs. (A2) and (A3) by using the radius of gyration and $L=2.60$ μm as reported previously.[5] Furthermore, the density of a B40 EPS melt was estimated as 1000 kg/m^3. In Fig. 6 it is shown that Δ has a value of 96 nm at $c_p<1$ g/ℓ, which nearly agrees with $\Delta=R_g$. Above this concentration, Δ decreases as a function of c_p as can be expected since $c_p^*=0.92$ g/ℓ. In the concentration region where we observe and calculate phase separation (from 0.3 to 1.5 g/ℓ), the decrease of Δ as a function of c_p can be neglected and Δ has a constant value. This means that we do not have to incorporate a $\Delta(c_p)$ dependence in our calculations.

[1] M. W. Beijernick, Zentralbl. Bakteriol. Parasitenkd. Infektionskr. 2 Abt. **2**, 697 (1896).
[2] V. B. Tolstoguzov, Food Hydrocolloids **4**, 429 (1991).
[3] V. B. Tolstoguzov, in *Food Colloids and Polymers: Stability and Mechanical Properties,* edited by E. Dickinson and P. Walstra (Royal Soc. Chem., Cambridge, 1992), Vol. 113, p. 94.
[4] Yu. A. Antonov, A. A. Soshinskii, and Yu. K. Glotova, Appl. Biochem. Microbiol. **30**, 760 (1994).
[5] R. Tuinier, P. Zoon, C. Olieman, M. A. Cohen Stuart, G. J. Fleer, and C. G. de Kruif, Biopolymers **49**, 1 (1999).
[6] C. G. De Kruif, Langmuir **8**, 2932 (1992).
[7] Th. J. M. Jeurnink and C. G. De Kruif, J. Dairy Sci. **60**, 139 (1993).
[8] I. Traube, Gummi-Ztg. **39**, 434 (1925).
[9] C. F. Vester, Kolloid-Z. **84**, 63 (1938).
[10] S. Asakura and F. Oosawa, J. Chem. Phys. **22**, 1255 (1954); Polym. Sci. **33**, 183 (1958).

[11] A. Vrij, Pure Appl. Chem. **48**, 471 (1976).
[12] H. De Hek and A. Vrij, J. Colloid Interface Sci. **84**, 409 (1981).
[13] H. N. W. Lekkerkerker, Colloids Surface **51**, 419 (1990).
[14] H. N. W. Lekkerkerker, W. C. K. Poon, P. N. Pusey, A. Stroobants, and P. B. Warren, Europhys. Lett. **20**, 559 (1992).
[15] W. C. K. Poon and P. N. Pusey, in *Observation and Simulation of Phase Transitions in Complex Fluids*, edited by M. Baus, L. F. Rull, and J-P. Ryckaert (Kluwer Academic, Dordrecht, 1995), p. 3.
[16] D. A. McQuarrie, *Statistical Mechanics* (Harper & Row, New York, 1976).
[17] J. Lyklema, *Fundamentals of Colloid and Interface Science* (Academic, New York, 1991), Vol. 1, Chap. 2.
[18] L. S. Ornstein and F. Zernike, Proc. K. Ned. Akad. Wet. **17**, 793 (1914).
[19] J. P. Hansen and I. R. McDonald, *Theory of Simple Liquids* (Academic, New York, 1976).
[20] M. J. Gillan, Mol. Phys. **38**, 1781 (1979).
[21] G. J. Fleer, J. M. H. M. Scheutjens, and B. Vincent, ACS Symp. Ser. **240**, 245 (1984).
[22] J. K. Percus and G. J. Yevick, Phys. Rev. **110**, 1 (1958).
[23] K. R. Hall, J. Chem. Phys. **57**, 2252 (1972).
[24] D. Frenkel and A. Ladd, J. Chem. Phys. **81**, 3188 (1981).
[25] R. J. Baxter, J. Chem. Phys. **49**, 2770 (1968).
[26] R. O. Watts, D. Henderson, and R. J. Baxter, Adv. Chem. Phys. **21**, 421 (1971).
[27] M. H. G. Penders and A. Vrij, Adv. Colloid Interface Sci. **36**, 185 (1991).
[28] R. Tuinier and C. G. de Kruif, in *Gums and Stabilisers for the Food Industry*, edited by P. A. Williams and G. O. Phillips, (Royal Society of Chemistry, Cambridge, 1998).
[29] B. Cichocki and B. U. Felderhof, J. Chem. Phys. **93**, 4427 (1990).
[30] R. Tuinier, P. Zoon, M. A. Cohen Stuart, G. J. Fleer, and C. G. de Kruif (unpublished).
[31] N. G. Hoogeveen, C. W. Hoogendam, R. Tuinier, and M. A. Cohen Stuart, Int. J. Polym. Anal. Charact. **1**, 315 (1995).
[32] R. I. Cukier, Macromolecules **17**, 252 (1984).
[33] P. G. De Gennes, Macromolecules **9**, 594 (1976).
[34] P. Tong, X. Ye, B. J. Ackerson, and L. J. Fetters, Phys. Rev. Lett. **79**, 2363 (1997).
[35] X. L. Chu, A. D. Nikolov, and D. T. Wasan, Langmuir **12**, 5004 (1996).
[36] S. M. Ilett, A. Orrock, W. C. K. Poon, and P. N. Pusey, Phys. Rev. E **51**, 1344 (1995).
[37] P. G. De Gennes, Macromolecules **14**, 1637 (1981); **19**, 492 (1982).
[38] J. M. H. M. Scheutjens and G. J. Fleer, J. Phys. Chem. **83**, 1619 (1979).
[39] J. M. H. M. Scheutjens and G. J. Fleer, J. Phys. Chem. **84**, 245 (1980).
[40] W. Kuhn, Kolloid-Z. **68**, 2 (1934).
[41] P. J. Flory, *Principles of Polymer Chemistry* (Cornell University Press, New York, 1953); *Statistical Mechanics of Chain Molecules* (Interscience New York, 1969).